PROCEEDINGS OF SPIE

SPIEDigitalLibrary.org/conference-proceedings-of-spie

Influence of extrinsic properties on magnetism and magnetotransport in Mn doped Bi2Te3 topological insulator with self-organized MnBi2Te4 layers

J. Sitnicka, K. Park, M. Konczykowski, K. Sobczak, J. Borysiuk, et al.

J. Sitnicka, K. Park, M. Konczykowski, K. Sobczak, J. Borysiuk, P. Skupiński, K. Grasza, Z. Adamus, A. Reszka, M. Tokarczyk, N. Olszowska, J. Kołodziej, B. J. Kowalski, L. Krusin-Elbaum, A. Wołoś, "Influence of extrinsic properties on magnetism and magnetotransport in Mn doped Bi2Te3 topological insulator with self-organized MnBi2Te4 layers," Proc. SPIE 12568, Metamaterials XIV, 1256804 (6 June 2023); doi: 10.1117/12.2666889



Event: SPIE Optics + Optoelectronics, 2023, Prague, Czech Republic

Influence of extrinsic properties on magnetism and magnetotransport in Mn doped Bi₂Te₃ topological insulator with self-organized MnBi₂Te₄ layers.

J. Sitnicka^a, K. Park^b, M. Konczykowski^c, K. Sobczak^d, J. Borysiuk^a, P. Skupiński^e, K. Grasza^e, Z. Adamus^e, A. Reszka^e, M. Tokarczyk^a, N. Olszowska^f, J. Kołodziej^{f,g}, B. J. Kowalski^e, L. Krusin-Elbaum^h, and A. Wołoś^{*a}

^aFaculty of Physics, University of Warsaw, ul. Pasteura 5, Warsaw, Poland; ^bDepartment of Physics, Virginia Tech, 850 West Campus Drive, Blacksburg, VA 24061, United States of America; ^cLaboratoire des Solides Irradiés, Ecole Polytechnique, CNRS, F-91128 Palaiseau, France; ^dFaculty of Chemistry, CNBCh, University of Warsaw, Zwirki i Wigury 101, Warsaw, Poland; ^eInstitute of Physics, PAS, Aleja Lotników 32/46, Warsaw, Poland;

^fNational Synchrotron Radiation Centre SOLARIS, Jagiellonian University, ul. Czerwone Maki 98, 30-392 Cracow, Poland; ^gFaculty of Physics, Astronomy and Applied Computer Science, Jagiellonian University, ul. prof. Stanisława Łojasiewicza 11, 30-348 Cracow, Poland;

^hDepartment of Physics, The City College of New York–CUNY, 85 St. Nicholas Terrace, New York, NY 10027, United States of America

ABSTRACT

Magnetic topological insulators are a new class of materials that combine magnetism with topology, which leads to exotic quantum phenomena such as the quantum anomalous Hall effect and the axion insulator phase. Of the magnetic topological insulators, those with MnBi₂Te₄ magnetic septuple layers self-assembled in a non-magnetic topological Bi₂Te₃ host material are of particular interest and have recently been extensively studied. Here, we present an overview of our recent advances in understanding the influence of several factors such as the ordering of Mn impurities, omnipresent magnetic disorder, and the position of the Fermi level on ferromagnetism and magnetotransport in such systems. In particular, the consequences of these effects for observation or lack of the quantized anomalous Hall effect are discussed. Both theoretical and experimental research on these issues is crucial for gaining controllable access to the quantum anomalous Hall effect and other spintronic phenomena, which have potential applications in low-power consumption electronic devices, data storage, and quantum computing.

Keywords: magnetic topological insulators, ferromagnetic resonance, magnetotransport, magnetism, electron irradiation, anomalous Hall effect, Berry curvature

1. INTRODUCTION TO MAGNETIC TOPOLOGICAL INSULATORS

Topological states of matter are different from their traditional classifications based on the phenomenological theory of Ginzburg-Landau phase transitions [1]. The defining characteristics of a topological state of quantum matter include the lack of a local order parameter, as described by the Ginzburg-Landau theory, and the presence of states that are not affected by the disorder [2]. The quantum Hall effect (QHE) is the first observed example of a topological state in condensed matter. The QHE state occurs when a two-dimensional (2D) electron system is under a high perpendicular magnetic field and electron orbits are quantized into Landau levels, engendering an insulating state with dissipationless, chiral currents flowing around the edges. The experimental results showing perfectly quantized Hall conductance (quantization was measured to an accuracy of $10^{-9} h/e^2$) were explained using the concept of topology from the Thouless-Kohmoto-Nightingale-den Nijs (TKNN) theory [3,4]. This theory describes a 2D electron system with broken time-reversal symmetry, and is characterized by a topological invariant called the Chern number (*C*) that can be directly derived from the Berry curvature integrated over the Brilloin zone, and is therefore an intrinsic property of the band structure. The integer quantum Hall conductivity σ_{xy} is expressed as $\sigma_{xy} = Ce^2/h$ where *e* is the electron charge and *h* is Planck's constant. Since *C* is an integer there is no way to deform the parameters of a material with $C \neq 0$ to connect it to a trivial insulator

Metamaterials XIV, edited by Vladimír Kuzmiak, Tomasz Stefaniuk, Kęstutis Staliūnas, Proc. of SPIE Vol. 12568, 1256804 ⋅ © 2023 SPIE ⋅ 0277-786X ⋅ doi: 10.1117/12.2666889

with C = 0 or to a vacuum (which also has C = 0). These edge channels provide a quantized Hall conductivity and are immune to backscattering, allowing for non-dissipative transport.

For a practical use of such edge transport though, a system implementing the quantum anomalous Hall effect (QAHE), a quantized version of the anomalous Hall effect (AHE), is desirable. It allows QHE states to prevail without a need for Landau levels formation which is only possible in high-mobility samples and under strong external magnetic fields [5,6]. With the discovery of three-dimensional topological insulators (TIs), it was realized that QAHE could exist if magnetization was introduced into them [7–9]. Thus, work began on a class of materials called magnetic topological insulators (MTIs). In contrast to the QHE state, the topological insulator phase occurs while maintaining time-reversal symmetry (TRS), hence it is described by a topological invariant other than the C number which is the Z_2 number [10–13]. It implements helical (spin-momentum locked) edge or surface states in 2D or 3D, respectively [14,15], that are robust against disorder. Without the introduction of magnetism, the 3D topological insulator has a gap in its bulk and gapless Dirac surface states that are protected by the TRS. However, if an out-of-plane magnetization is introduced into the system, the TRS will be broken and energy gaps will open on the top and bottom surfaces turning each of them into a phase with a non-zero Chern number [7–9]. Thus, at the interface between the gapless side surface and the top/bottom surface, half-quantized, chiral edge channels will be trapped, each with a conductivity of $\sigma_{xy} = e^2/(2h)$. In order to realize QAHE the Fermi level should be positioned within the bulk band gap as well as the surface band gap. This excludes all the conductivity from the bulk and the inner area of the surfaces.

* agnieszka.wolos@fuw.edu.pl

2. Bi₂Te₃ DOPED WITH Mn AND THE OCCURRENCE OF SELF-ORGANIZED MnBi₂Te₄

Doping with magnetic impurities is a convenient approach to introduce magnetism into TIs [16–19], which owes its success to the knowledge gained from studies of dilute magnetic semiconductors [20,21]. One of the systems widely used to realize emergent exotic quantum phenomena is the topological insulator bismuth telluride (Bi₂Te₃) doped with manganese (Mn). The layered crystal structure of Bi₂Te₃ allows manganese atoms to enter random positions in the lattice, which results in different magnetic properties of this system. At low doping, Mn preferentially replaces Bi sites, while increased doping causes Mn to enter interstitial positions in van der Waals gaps [16,22,23]. Under appropriate growth conditions, Mn ions can form self-organized heterostructures composed of an alternating sequence of MnBi₂Te₄ septuple layers (SLs) and *n* - fold Bi₂Te₃ quintuple layers (QLs) (Fig. 1a-c). The MnBi₂Te₄/(Bi₂Te₃)_n compounds belong to the family of intrinsic magnetic topological insulators (IMTIs) which, compared to dilute magnetic topological insulators (DMTIs) with randomly distributed Mn atoms, can provide larger Dirac mass gap as well as an increase in the QAHE realization temperature [24–26]. The QAHE state has been indeed achieved in crystal flakes with the MnBi₂Te₄/(Bi₂Te₃)_n naturally occurring superlattice at record-high temperature [27] and it became simultaneously clear that the reduction of the influence of extrinsic effects such as magnetic disorder caused by different locations of Mn dopants is necessary to master the effect.

In this work in Chapter 3 we will present our contribution to the understanding of the magnetic disorder in MnBi₂Te₄/(Bi₂Te₃)_n. In Chapter 4 we will discuss the influence of the position of the Fermi level on magnetic and magnetotransport properties, which is another important issue to understand and control the QAHE. An in-depth analysis of each of the above issues is presented in the dedicated papers [28,29].

3. DISORDER IN MnBi₂Te₄/(Bi₂Te₃)_n AND ITS INFLUENCE ON MAGNETISM AND SURFACE BAND STRUCTURE

It has been established that the intra-layer ordering within a model MnBi₂Te₄ single layer is ferromagnetic (FM) with phase transition temperature of about 12 K [30]. Three-dimensional MnBi₂Te₄ has an A-type antiferromagnetic (AFM) structure: every ferromagnetic SL with an out-of-plane easy magnetic axis is weakly antiferromagnetically coupled with neighboring SLs. The interlayer coupling stabilizes bulk AFM phase with the Neel temperature 25 K. The interlayer coupling is tunable via intercalation of non-magnetic Bi₂Te₃ QLs, forming a family of MnBi₂Te₄/(Bi₂Te₃)_n with rich topological and physical properties [25,31–35]. The MnBi₂Te₄/(Bi₂Te₃)_n with n = 1-3 show effects of interlayer decoupling manifested by a strong drop of Neel temperature with increased distance between SLs, from 25 K for n = 0 down to 13 K for n = 1 and 11.9 K for n = 2 [33]. For $n \ge 3$ the vanishing exchange coupling between SLs is theoretically predicted [33,34], however samples with n > 3 show FM behavior indicating the presence of another mechanism that can couple SLs at higher distances [27,33].

The key to controlling the topological phases in the MnBi₂Te₄ family of compounds is to design their interlayer magnetic coupling. However, in addition to tuning interlayer interactions by changing the number of separating QLs or lattice engineering by using pressure [36] or chemical substitution [37], one should not forget that there exist inherent disorder in these systems that can independently affect their magnetism. Our studies [28] performed on ferromagnetic samples of MnBi₂Te₄/(Bi₂Te₃)_n grown by the Bridgman method with different distance n between adjacent SLs and the Curie temperature T_C ranging between 6 K and 13 K (for details see methods in [28]) has shown two types of disorder. The first one is related to the broadly understood distribution of SLs and QLs, which include the statistical distribution of QLs, grouping of SLs in a superlattice containing multiples of mostly three SLs or break in the continuity of SLs where SLs interchange with QLs (Fig. 1 c). The second type of disorder, which seems to be crucial to the magnetic properties of the MnBi₂Te₄/(Bi₂Te₃)_n samples, is the distribution of Mn between SLs and QLs. Micro-chemical analysis performed by energy dispersive x-ray measurements (EDX) has revealed a dearth of Mn in SLs and a simultaneous presence of Mn in otherwise non-magnetic QLs (Fig. 1 d-e). In the depleted SLs the concentration of Mn may be reduced down to 4.4 +/- 0.7 at. %, compared to 14 at. % in the nominal MnBi₂Te₄. This entails a decrease in the Curie temperature to 6 K (for comparison, the Curie temperature of a single but ideal MnBi₂Te₄ layer is 12 K). Samples showing the highest concentration of Mn in SLs, 10.6 +/- 1.6 at. %, which is within the three sigma limit to the nominal concentration, simultaneously show the highest T_c , suggesting that the disorder in SLs is the most important factor influencing phase transition temperature in MnBi₂Te₄/(Bi₂Te₃)_n. It is worth noting, that samples with a low disorder in SLs are required in order to observe QAHE in a high-temperature regime [27].

Along with the disorder in the septuple layers, there is a disorder in Bi₂Te₃ quintuple layers. As mentioned before, Mn is doped into Bi₂Te₃, most probably substituting Bi site. We have found between 0.3 and 1 at. % of Mn in Bi₂Te₃ QLs of the MnBi₂Te₄/(Bi₂Te₃)_n heterostructure [28]. The presence of Mn in Bi₂Te₃ changes the nature of the MnBi₂Te₄/(Bi₂Te₃)_n system. MnBi₂Te₄ are no longer independent non-interacting layers at large distances *n*. Instead, they become coupled via a sparse population of Mn in QLs. Indeed, in the ferromagnetic resonance experiment, we observed the splitting of the resonance line into the acoustic and the optical modes of the coupled SL and Mn-doped QL spin subsystems, which will be described below.

The magnetic resonance in two coupled ultra-thin films consists of two eigenmodes formed by the uniform modes of the individual layers, the acoustic mode for which the magnetization precession of both films occurs in-phase and the weaker optical mode where the mutual precession is out-of-phase [38–40]. The acoustic and optical modes of the coupled SL and Mn doped QL spin subsystems are clearly resolved at low temperatures for MnBi₂Te₄/(Bi₂Te₃)_n samples with the highest T_C and the lowest line width, Figure 2a-b. The stronger acoustic mode is located at a higher magnetic field than the weaker optical mode thus indicating the FM coupling between the layers. The small difference in the amplitude and in the position of the two modes indicates a small value of the inter-layer coupling parameter which was estimated at $J = 1.37 \times 10^{-7}$ J m⁻² (see phenomenological analysis of FMR in [28]).

In most of the studied samples, however, due to the broadening of the resonance line and small inter-layer coupling leading to the small separation of the component lines, a single asymmetric resonance line is typically observed. In such case, the system can be treated with a uniform mode approximation, neglecting the FMR line splitting, Figure 2c. With this assumption, the magnetic anisotropy constants can be described as the magnetization-weighted mean values of the two spin subsystems as discussed by [38].

With the above approximation and since the MnBi₂Te₄/(Bi₂Te₃)_n is an out-of-plane easy axis system [28], the difference between the FMR resonance field for the magnetic field H applied parallel to the c-axis $(H_{res}(0^o))$ and perpendicular to it $(H_{res}(90^{\circ}))$ is three times the anisotropy field (see the free energy in [28]):

$$H_{res}(0^o) - H_{res}(90^o) = 3H^A.$$
 (1)

 $H_{res}(0^o) - H_{res}(90^o) = 3H^A$. (1) The magnetic anisotropy field H^A calculated using the above relation is shown in Figure 2d as a function of temperature. The H^A decreases with increasing temperature, vanishing gradually with a long tail extending above T_C due to the magnetic correlations that survive to the paramagnetic phase. Both the magnitude of the magnetic anisotropy field H^A and the T_C (determined from the magnetotransport studies [28]) correlates with the quality of a SL. The highest magnetic anisotropy, reaching ~ 0.3 T at 5 K ($T_C = 13$ K) was obtained for the sample with the evaluated concentration of Mn in SLs equal to about 10.6 at.%, while the lowest magnetic anisotropy was ~ 0.15 T at 5 K and $T_C = 6$ K, for the sample with the greatest deviation from the ideal structure, only 4.4 at.% of Mn in SLs (Fig. 2d). The magnetic quality of SLs seems to play an overriding role, and since other disorder effects also exist (the most striking is doping of Mn into Bi₂Te₃ and statistical distribution of the distances between SLs) the resulting T_C must be a combined effect of these disorder metrics.

Disorder in SLs has also a detrimental effect on the surface band structure. It has been studied by angle-resolved photoemission spectroscopy (ARPES) and density functional theory (DFT) in [28]. In the DFT calculated band structure of MnBi₂Te₄/(Bi₂Te₃)_n corresponding to a 2QL-SL-terminated surface where 50 % of Mn in a SL was replaced by Bi, characteristic features can be seen which are not present for perfect structures, Figure 3a. The Dirac cone appears to be split into a peculiar double structure (TSS1 and TSS2) and there appears an extra broad parabolic conduction band (CB). The wave functions of the individual energy bands can be no longer assigned to the respective component layers, as it is in the case of ideal MnBi₂Te₄/(Bi₂Te₃)_n where typically at least 40 % of the electron density is localized at the specific QLs or SLs [28]. Instead, the wave functions are delocalized between the component layers. Figure 3a shows states in which at least 28 % of the electron density is localized at the topmost QL in a disordered structure. This disordered band structure has been confirmed in ARPES, Figure 3b-f. Doubling of the Dirac cone and presence of the broad parabolic band as well as the lack of the magnetic gap (which appears solely on the SL-terminated surface) are evident in Fig. 3b. In Fig. 3c-f, constant energy contours recorded at 24 eV photon energy are shown. Topological surface states (TSSs) show hexagonal flower-shaped pattern, which contrasts to the star-like warped surface states in pristing Bi₂Te₃ [41,42] and has been earlier linked to the hybridization of the outermost QL with underlying SL even in the perfect structure [43]. A disordered crystal, which band structure is shown in Fig. 3b-f, despite relatively high T_c equal to 10 K and nice macroscopic structure revealing a shiny c plane, is not suitable for the realization of the QAHE.

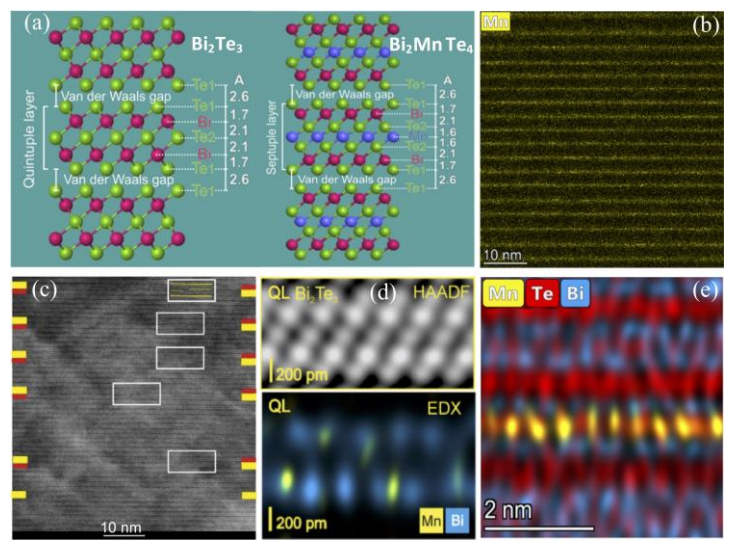


Figure 1 (a) The structure of Bi₂Te₃ composed of quintuple layers and Bi₂MnTe₄ composed of septuple layers. Bi atoms are shown in red, Te in green, and Mn in blue, respectively. Manganese is planarly incorporated into the middle of a SL. The SLs and QLs are separated by van der Waals gaps. (b) EDX mapping of MnBi₂Te₄/(Bi₂Te₃)_n superlattice with the distribution of Mn atoms shown in yellow. (c) Scanning transmission electron microscopy image showing a break in the continuity of SLs where SLs interchange with QLs. Yellow blocks denote SLs and red blocks mark QLs. (d) High-angle annular dark field scanning transmission electron microscopy (HAADF-STEM) image and EDX mapping demonstrate Mn atoms substituting Bi sites in a QL. (e) High-resolution EDX mapping of Mn in a SL. The quantitative analysis reveals a dearth of Mn in SLs. [(d) copyright IOP]

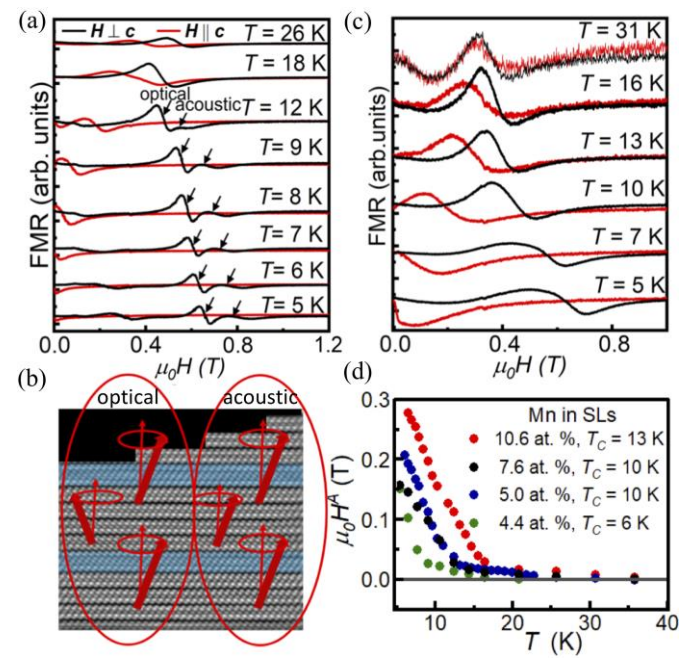


Figure 2. (a) The FMR spectra of the high-quality MnBi₂Te₄/(Bi₂Te₃)_n sample showing a separation of the acoustic and optical resonance modes of the coupled SLs and Mn doped QLs. (b) Schematic presentation of magnetic coupling between SLs (marked in blue) and sparse population of Mn in adjacent QLs (grey). The acoustic mode arises when precession of the magnetic moments (marked with red thick arrows) of the component layers around the direction of the external magnetic field (marked with red thin arrows) is in-phase, the optical mode arises for the out-of-phase precession. (c) FMR of disordered MnBi₂Te₄/(Bi₂Te₃)_n. A broadened single resonance line is visible. (d) The anisotropy field determined from equation (1) versus temperature for samples with different concentrations of Mn in SLs. Each sample is also labeled with its T_C determined from the magnetotransport studies. The sample with the highest concentration of Mn in SLs shows the highest anisotropy field and simultaneously the highest T_C . [(c) and (d) copyright IOP]

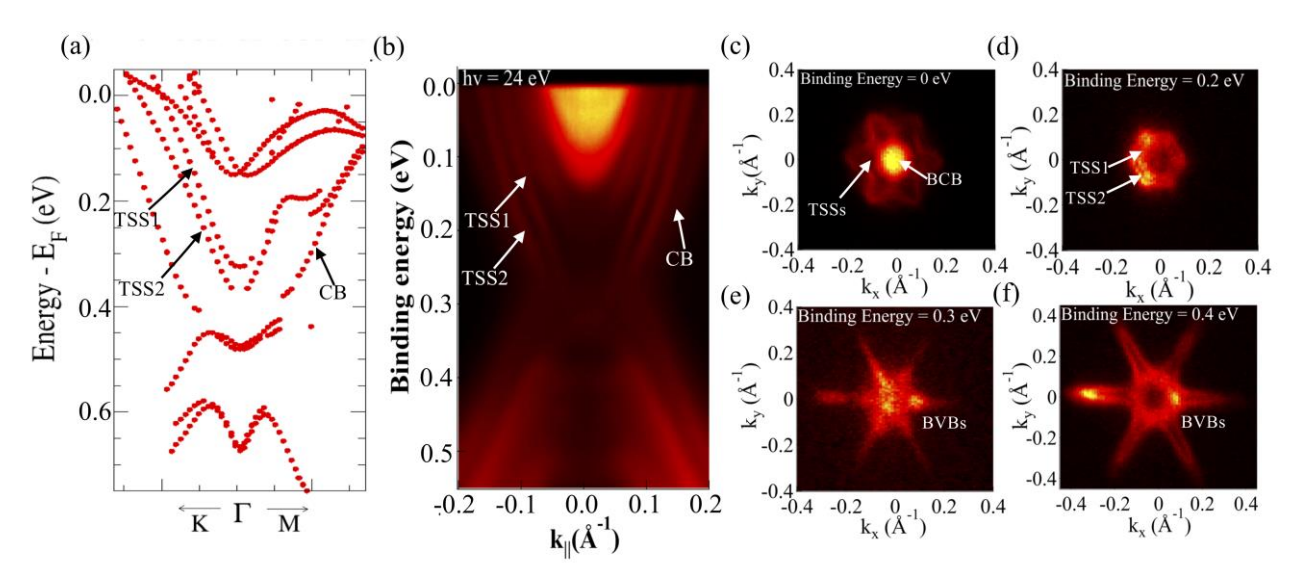


Figure 3. (a) Band structure DFT calculations of a 2QL-SL-2QL-SL slab where 50 % of Mn atoms in SLs were replaced by Bi. In (a) only the states where at least 28% of the electron density is localized at the topmost QL are shown, in order to relate the calculations to the ARPES spectra (probing depth in ARPES is ~ 1 nm which is roughly the width of a single QL or SL). Split Dirac cone into TSS1 and TSS2 and broad parabolic conduction band CB is marked with arrows. (b) ARPES spectra of disordered MnBi₂Te₄/(Bi₂Te₃)_n collected along $\Gamma \rightarrow M$ direction at 6 K and at photon energy hv = 24 eV. All the most pronounced features of the modeled structure in (a), TSS1, TSS2 and CB, are revealed in the ARPES experiment. (c) - (f) Constant energy contours maps from ARPES measurements at different binding energies at hv = 24 eV. BCB stays for the bulk conduction band and BVB stays for the bulk valence band, respectively. [(a) and (b) copyright IOP]

4. INFLUENCE OF FERMI LEVEL IN MnBi₂Te₄/(Bi₂Te₃)_n ON MAGNETISM AND MAGNETOTRANSPORT

The QAHE reported in [27] has been observed in a new regime of conducting bulk. The quantization of the surface conductivity was revealed, among other factors, thanks to the vanishing bulk anomalous Hall effect. In general, three regimes of the AHE are typically distinguished in the bulk: clean limit with dominating extrinsic skew scattering mechanism proportional to the transport lifetime leading therefore to the proportionality of the anomalous Hall conductivity σ_{xy}^{AHE} to the longitudinal conductivity σ_{xx} , $\sigma_{xy}^{AHE} \propto \sigma_{xx}$; intermediate regime with suppressed skew scattering mechanism and dominating intrinsic Berry phase-driven mechanism with σ_{xy}^{AHE} independent on σ_{xx} ; and finally dirty regime with hopping conductivity leading to $\sigma_{xy}^{AHE} \propto \sigma_{xx}^{\beta}$ with $\beta = 1.6$ - 1.8 [44–46]. In the case of high-quality MnBi₂Te₄/(Bi₂Te₃)_n, either *n*-type [27] or *p*-type [29], it turns out that the dominating mechanism for AHE has an intrinsic nature. Moreover, theoretical considerations [27,46] showed that the Berry phase is concentrated near the avoided band crossings. Indeed, in MnBi₂Te₄/(Bi₂Te₃)_n we have observed non-monotonic dependence of the AHE on the Fermi level tuned by the electron irradiation [29]. The dependence of the sample magnetization on the Fermi level, and thus a possible RKKY interaction, has been ruled out, suggesting that the observed non-monotonic dependence of the AHE must solely originate from the Berry phase profile (for details see [29]).

Figure 4a shows the anomalous Hall conductivity σ_{xy}^{AHE} of the ferromagnetic MnBi₂Te₄/(Bi₂Te₃)_n sample, pristine and irradiated with 2.5 MeV electron beam. Before irradiation, sample is *p*-type with hole concentration $p = 1.8 \times 10^{20}$ cm⁻³, and does not show the AHE. The AHE appears after electron irradiation and tuning the Fermi level E_F to the conduction band with $n = 7.6 \times 10^{16}$ cm⁻³. The AHE increases by a factor of two when the electron concentration is increased to $n = 8.9 \times 10^{16}$ cm⁻³. This is consistent with the non-linear scaling of the AHE with the position of the E_F [29] due to the Berry phase, which is non-zero only close to the top of the valence band/bottom of the conduction band. Figure 4b shows the σ_{xy}^{AHE} measured versus magnetic field *H* at different temperatures, showing a rapid decrease of the σ_{xy}^{AHE} at the critical temperature T_c equal to 13 K. The T_c does not change upon irradiation, see discussion in [29].

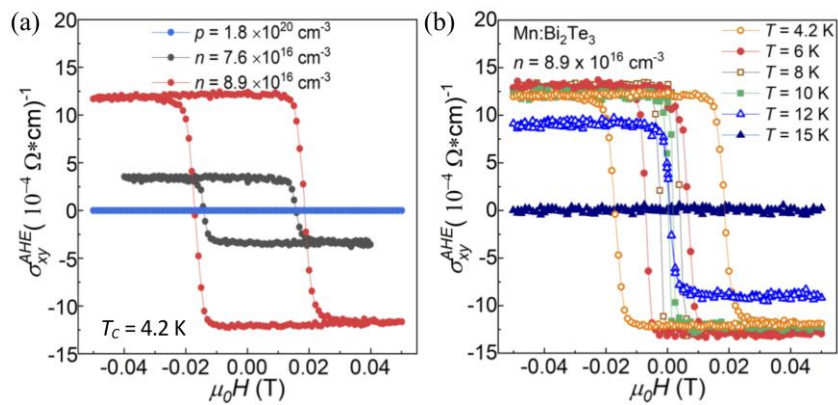


Figure 4. (a) σ_{xy}^{AHE} vs. out-of-plane H for pristine and irradiated MnBi₂Te₄/(Bi₂Te₃)_n samples measured at 4.2 K. σ_{xy}^{AHE} is null in the pristine p-type sample and appears after converting sample to n-type by electron irradiation. (b) σ_{xy}^{AHE} measured versus H at different T shows a rapid drop of σ_{xy}^{AHE} near T_c , between 12 and 15 K.

5. CONCLUSIONS

Magnetic disorder as well as the concentration of free carriers are indispensable extrinsic properties of MnBi₂Te₄/(Bi₂Te₃)_n that are challenging to reproduce in a controlled manner and can vary greatly depending on the growth procedure. That is why it is so important to thoroughly understand their influence before proceeding with controlled modifications of self-organized MnBi₂Te₄/(Bi₂Te₃)_n structures.

Our studies show that there is an omnipresent migration of Mn between SLs and quintuple layers: Mn is often missing in SLs and substitutes into QLs. Ferromagnetic resonance studies show that the depleted SLs couple via an available population of Mn in QLs and the system is ferromagnetically stabilized in three dimensions. Moreover, the disorder effects significantly change the surface electronic band structure and all electron states that are well assigned to respective energy bands and simultaneously localized on respective QLs or SLs in perfect structures, in disordered material become delocalized.

We have also investigated the dominant contribution to the bulk AHE in Mn-doped Bi₂Te₃ containing SLs. The main AHE effect arises from the intrinsic Berry-phase driven mechanism, which exhibits non-linear scaling with the position of the Fermi level, consistent with recent findings [27] that the non-quantized anomalous Hall conductivity quickly approaches zero when the Fermi level moves from the top into the valence band (or from the bottom into the conduction band). This is due to the property of the Berry curvature, which is concentrated near avoided band crossings. We managed to experimentally show for the first time the non-monotonic dependence of AHE on the position of the Fermi level in the intrinsic mechanism.

Concurrently, our findings on the influence of the position of the Fermi level on magnetism in Mn-doped Bi₂Te₃ with SLs exclude a carrier-mediated mechanism in ferromagnetic ordering. Thus magnetic TIs with SLs constitute distinct magnetic systems from widely studied diluted magnetic topological insulators samples.

In conclusion, there are two distinct disorder effects that dominate magnetic properties of the MnBi₂Te₄/(Bi₂Te₃)_n system. One is the location of Mn dopants randomly distributed among SLs and QLs that can deny the observation of QAHE by destroying the surface band structure. Two, the disorder in MnBi₂Te₄ leads to the lowering of the critical phase transition temperature. On the other hand, a presence of Mn in Bi₂Te₃ quintuple layers coupling SLs in 3D does not disturb QAHE which has been successfully observed in [27]. The dominating intrinsic mechanism for the non-quantized AHE related to the Berry phase quenches the AHE deep in the conduction/valence bands allowing the observation of the quantization in the surface electric transport. All in all, even in the presence of the ubiquitous disorder, MnBi₂Te₄/(Bi₂Te₃)_n displays a relatively high mobility, of the order of 1000 cm²/(Vs), which prevents it from entering the dirty hopping regime.

Magnetic TIs with SLs show rich physics that still requires in-depth study. Our research certainly brings us closer to obtaining controlled access to the magneto-topological phenomena in these systems, in particular to the much-anticipated quantum anomalous Hall effect.

ACKNOWLEDGMENTS

This work was supported by the Polish National Science Center grant 2016/21/B/ST3/02565.

REFERENCES

- [1] Landau, L. D. and Lifshitz, E. M., Statistical Physics Part 2 volume 9, Robert Maxwell M. C Publisher, Pergamon Press (1981).
- [2] J. Maciejko, T. L. Hughes, and S.-C. Zhang, "The Quantum Spin Hall Effect," Annu. Rev. Condens. Matter Phys., 31-53 (2011).
- [3] Thouless, D. J., Kohmoto, M., Nightingale, M. P., and den Nijs, M., "Quantized Hall Conductance in a Two-Dimensional Periodic Potential," Phys. Rev. Lett. 49, 405-408 (1982).
- [4] Kohmoto, M. "Topological Invariant and the Quantization of the Hall Conductance," Ann. Phys 160, 343-354 (1985).
- [5] Haldane, F. D. M., "Model for a Quantum Hall Effect without Landau Levels: Condensed-Matter Realization of the "Parity Anomaly," Phys. Rev. Lett. 61, 2015-2018 (1988).
- [6] Onoda, M. and Nagaosa, N.," Quantized Anomalous Hall Effect in Two-Dimensional Ferromagnets: Quantum Hall Effect in Metals," Phys. Rev. Lett. 90, 206601-4 (2003).
- [7] Yu, R., Zhang, W., Zhang, H.-J., Zhang, S.-C., X. Dai, Fang, Z., "Quantized anomalous Hall effect in magnetic topological insulators," Science 329, 61-64 (2010).
- [8] Chu, R. L., Shi, J. and Shen, S. Q., "Surface edge state and half-quantized Hall conductance in topological insulators Rui-Lin," Phys. Rev. B 84, 0853121-5 (2011).
- [9] Tokura, Y., Yasuda, K. and Tsukazaki, A. "Magnetic topological insulators," Nat. Rev. Phys., 126 143 (2019).
- [10] Kane, C. L. and Mele, E. J., "Z₂ Topological Order and the Quantum Spin Hall Effect," Phys. Rev. Lett. 95, 146802(1)-4 (2005).
- [11] C. L. Kane and E. J. Mele, "Quantum Spin Hall Effect in Graphene," Phys. Rev. Lett. 95, 226801(1)-4 (2005).
- [12] Fu, L. and Kane, C. L., "Topological insulators with inversion symmetry," Phys. Rev. B 76, 045302(1)-17 (2007).
- [13] Fu, L., Kane, C. L. and Mele, E. J., "Topological Insulators in Three Dimensions," Phys. Rev. Lett. 98, 106803(1)-4 (2007).
- [14] König, M. Wiedmann, M. S., Brüne, C., Roth, A., Buhmann, H., Molenkamp, L. W., Qi, X. L., Zhang, S. C.," Quantum Spin Hall Insulator State in HgTe Quantum Wells" Science 318, 766-770 (2007).
- [15] Zhang, H., Liu, C. X., Qi, X. L., Dai, X., Fang, Z. and Zhang, S. C. "Topological insulators in Bi₂Se₃, Bi₂Te₃ and Sb₂Te₃ with a single Dirac cone on the surface," Nat. Phys. 5, 438-442 (2009).
- [16] Hor, Y. S. et al., "Development of ferromagnetism in the doped topological insulator Bi_{2-x}Mn_xTe₃," Phys. Rev. B 81, 195203(1)-7 (2010).
- [17] Dyck, J. S., Hájek, P., Lošťák P. and Uher, C., "Diluted magnetic semiconductors based on $Sb_{2-x}V_xTe_3$ (0.01 $\leq x \leq 0.03$)." Phys. Rev. B 65, 115212(1)-7 (2002).
- [18] Dyck, J. S., Hájek, P., Lošťák P. and Uher, C., "Low-temperature ferromagnetic properties of the diluted magnetic semiconductor Sb_{2-x}Cr_xTe₃" Phys. Rev. B 71, 115214(1)-6 (2005).
- [19] Chi, H., Tan, G., Kanatzidis, M. G., Li, Q., and Uher, C., "A low-temperature study of manganese-induced ferromagnetism and valence band convergence in tin telluride," Appl. Phys. Lett. 108, 182101(1)-5 (2016).
- [20] Kacman, P., "Spin interactions in diluted magnetic semiconductors and magnetic semiconductor structures" Semicond. Sci. Technol. 16, R25-R39 (2001).
- [21] Dietl, T. and Ohno, H. "Ferromagnetic III V and II VI," MRS Bull. 714-719 (2003).
- [22] A. Wolos et al., "High-spin configuration of Mn in Bi₂Se₃ three-dimensional topological insulator" J. Magn. Magn. Mater. 419, 301-308 (2016).
- [23] Růžička J. et al., "Structural and electronic properties of manganese- doped Bi₂Te₃ epitaxial layers" New J. Phys. 17, 013028(1)-11 (2015).
- [24] Otrokov, M. M., Menshchikova, T. V., Rusinov, I. P., Vergniory, M. G., Kuznetsov, V. M. and Chulkov, E. V. "Magnetic extension as an efficient method for realizing the quantum anomalous hall state in topological insulators," JETP Lett. 105, 297-302 (2017).
- [25] Li, J., Li, Y., Du, S., Wang, Z., Gu, B.L, Zhang, S. C., He, K., Duan, W. and Xu, Y., "Intrinsic magnetic topological insulators in van der Waals layered MnBi₂Te₄-family materials" Sci. Adv. 5, 1-7 (2019).
- [26] Chi, H. and Moodera, J. S. "Progress and prospects in the quantum anomalous Hall effect," APL Mater. 10, 090903(1)-13 (2022).
- [27] Deng, H., et al., "High-temperature quantum anomalous Hall regime in a MnBi₂Te₄/Bi₂Te₃ superlattice," Nat. Phys. 17, 36-42 (2021).
- [28] Sitnicka, J. et al., "Systemic consequences of disorder in magnetically self-organized topological

- MnBi₂Te₄/(Bi₂Te₃)_n superlattices," 2D Mater. 9, 015026(1)-12 (2022).
- [29] Sitnicka, J., Konczykowski, M., Sobczak, K., Skupiński, P., Grasza, K., Adamus, Z., Reszka, A. and Wołoś, A., "Fermi level dependence of magnetism and magnetotransport in the magnetic topological insulators Bi₂Te₃ and BiSbTe₃ containing self-organized MnBi₂Te₄ septuple layers," arXiv:2211.00546 (2022).
- [30] Otrokov, M. M, Rusinov, I.P, Blanco-Rey, M., Hoffmann, M., Vyazovskaya, A., Y, Eremeev, S. V., Ernst, A., Echenique, P. M., Arnau, A. and Chulkov, E. V." Unique Thickness-Dependent Properties of the van der Waals Interlayer Antiferromagnet MnBi₂Te₄Films," Phys. Rev. Lett. 122, 107202(1)-6 (2019).
- [31] Gong, Y., et al., "Experimental Realization of an Intrinsic Magnetic Topological Insulator," Chinese Phys. Lett. 36, 076801(1)-6 (2019).
- [32] Otrokov M. M, et al., "Prediction and observation of an antiferromagnetic topological insulator," Nature 576, 416 437 (2019).
- [33] Klimovskikh, I. I. et al., "Tunable 3D/2D magnetism in the (MnBi₂Te₄)(Bi₂Te₃)_m topological insulators family" Npj Quantum Mater., 1-9 (2020).
- [34] Wu, J., Liu, F., Liu, C., Wang, Y., Li, C., Lu, Y., Matsuishi, S., Hosono, H. "Toward 2D Magnets in the (MnBi₂Te₄)(Bi₂Te₃)_n Bulk Crystal," Adv. Mater. 32, 2001815(1)-7 (2020).
- [35] Ning, W. and Mao, Z. "Recent advancements in the study of intrinsic magnetic topological insulators and magnetic Weyl semimetals," APL Mater. 8, 090701(1)-9 (2020).
- [36] Shao, J. et al., "Pressure-Tuned Intralayer Exchange in Superlattice-Like MnBi₂Te₄/(Bi₂Te₃)_n Topological Insulators" Nano Lett. 21, 5874-5880 (2021).
- [37] Liu, Y., et al., "Site Mixing for Engineering Magnetic Topological Insulators," Phys. Rev. X 11, 021033(1)-12 (2021).
- [38] Heinrich, B. and Cochran, J. F., "Ultrathin metallic magnetic films: magnetic anisotropies and exchange interactions" Adv. Phys. 42, 523-639 (1993).
- [39] Lindner, J and Baberschke, K. "Ferromagnetic resonance in coupled ultrathin films," J. Phys. Condens. Matter 15, S465-S478 (2003).
- [40] Zhang, Z., Zhou, L. and Wigen, P.E., "Angular dependence of ferromagnetic resonance in exchange-coupled Co/Ru/Co trilayer structures," Phys. Rev. B 50, 6094-6112 (1994).
- [41] Chen, C., et al., "Experimental Realization of a Three-Dimensional Topological Insulator, Bi₂Te₃" *Science* 325, 178-180 (2009).
- [42] Chen, C., et al., "Robustness of topological order and formation of quantum well states in topological insulators exposed to ambient environment" *PNAS* **109**, 3694-3698 (2012).
- [43] Wu, X., et al., "Distinct Topological Surface States on the Two Terminations of MnBi₄Te₇," *Phys. Rev.* X 10, 031013(1)-10 (2020).
- [44] Nagaosa, N., Sinova, J., Onoda, S., MacDonald, A. H. and Ong, N. P. "Anomalous Hall effect", Rev. Mod. Phys. 82,1539-1592 (2010).
- [45] Onoda, M and Nagaosa, N., "Topological Nature of Anomalous Hall Effect in Ferromagnets" J. Phys. Soc. Japan 71, 19-22 (2002).
- [46] Xiao, D., Chang, M. C. and Niu, Q. "Berry phase effects on electronic properties," Rev. Mod. Phys. 82, 1959-2007 (2010).